

Article

# Size-Controlled Transparent Jute Fiber for Replacing Transparent Wood in Industry Production Area

Tianshi Feng <sup>1,†</sup>, Jiankun Qin <sup>1,2,†</sup>, Yali Shao <sup>1,2</sup>, Lili Jia <sup>1</sup>, Qi Li <sup>1,2</sup> and Yingcheng Hu <sup>1,2,\*</sup>

<sup>1</sup> College of Material Science and Engineering, Northeast Forestry University, Harbin 150040, China

<sup>2</sup> Key Laboratory of Bio-Based Material Science and Technology of Ministry of Education of China, College of Material Science and Engineering, Northeast Forestry University, Harbin 150040, China

\* Correspondence: yingchenghu@nefu.edu.cn; Tel.: +86-451-8219-0394

† These authors contributed equally to this work.

Received: 15 May 2019; Accepted: 6 July 2019; Published: 10 July 2019



**Abstract:** Transparent jute fiber (TJF) was prepared from delignified jute fiber (DJF) and was subjected to various surface knitting densities (190 and 340 g/m<sup>2</sup>) before epoxy resin (ER) impregnation under vacuum. The preparation process and properties of TJF were evaluated. The mechanical properties and surface morphology of the jute fiber samples were also studied. The mechanical properties were compared with transparent coir fiber (TCF) and transparent balsa wood (TBW). Optical properties, such as surface color, optical transmittance, and visual haze, of natural jute fiber (JF) and TJF were measured to better understand the influence of delignification. The experimental results showed transparency of 51% even for dense jute fiber cloth, and the maximum transmittance was as high as 60% with a low surface density. TJF had similar tensile strength as TBW but was higher than TCF, indicating a maximum tensile strength of 43.25 MPa with a surface density of 340 g/m<sup>2</sup>. These results suggest that TJF has the potential to meet the particular optical and mechanical properties of transparent wood. Transparent jute fiber can replace transparent wood for industrial production because of the simple preparation process and lower price.

**Keywords:** transparent jute fiber; epoxy resin; transmission; tensile strength; chromatic aberration

## 1. Introduction

A new biomass material called transparent wood has attracted widespread attention [1,2]. Transparent wood is a polymer material with a matched refractive index as delignified wood or modified wood with lignin, thus giving it optical properties and improving its mechanical properties [3]. The characteristic of transparent wood is that high transmittance and high haze exist side by side; thus, it is considered an excellent substitute for glass [4]. Power consumption of a building has always occupied a large proportion of total power consumption [5]. Therefore, if we could make full use of natural light to change the indoor lighting environment, we would save energy. Glass is widely used as a good transparent material, but the fragility of glass, the poor insulation effect, high energy consumption during construction, and other glass defects result in pollution. If transparent wood were used instead of glass as a light-guided material in modern intelligent buildings, the building would receive natural light under the premise of protecting privacy [6] and reduce the energy consumption of heating and cooling. Because transparent wood retains the original structure of wood, its texture can also be retained, resulting in a “visual force”, which is conducive to good physical and mental health and improving the comfort of residents [7].

A new kind of transparent wood with good near-infrared shielding ability and high visible light transmittance is available, which is made by dispersing nano-Cs<sub>x</sub>WO<sub>3</sub> in PMMA and filling delignified wood raw materials with it. Transparent wood with nano-Cs<sub>x</sub>WO<sub>3</sub> has excellent mechanical

properties, as its fracture strength is 59.8 MPa [8]. By removing lignin from 1 mm basswood with a NaOH/Na<sub>2</sub>SO<sub>3</sub> and H<sub>2</sub>O<sub>2</sub> system, a new transparent basswood with 90% transmittance and 80% haze was prepared. Then, the transparent wood was used as a cover for solar cells instead of glass [9]. As a result, photoelectric conversion efficiency increased by about 18%. A new kind of transparent wood with fluorescent properties was prepared by compounding transparent wood with CdTe fluorescent quantum dots. This wood would be useful in luminous buildings or in furniture [10]. Multilayered transparent wood with good mechanical properties and uniform fluorescence was prepared by laminating 0.6–0.8 mm balsawood at 45° and 90°, in accordance with the grain direction and adding fluorescent quantum dots [11]. A new method aimed to use sodium chlorite to remove lignin from poplar wood, and then place the product in a particular concentration of hydrogen peroxide solution and boil for 4 h. Then, the sample was rinsed with distilled water, vacuum-dried at 45 °C for 24 h, and combined with nano-Fe<sub>3</sub>O<sub>4</sub> particles to prepare transparent wood with good conductivity and magnetism [12]. However, those researchers did not consider the delignification process in detail, which resulted in a long processing time, a waste of pharmaceutical and experimental resources, and increased complexity of the experiment. The relationship between lignin, transmittance, and tensile strength has been reported for delignified basswood at different times. The experimental results show that by treating the wood fibers, transparent wood with low thermal conductivity and controllable size can be prepared [13]. Some researchers built a mini-cabin with transparent wood fibers instead of glass and found that the transparent wood fibers had a better thermal insulation effect than glass [14].

However, wood itself is an anisotropic heterogeneous material, and various defects easily form during the growth process. Some shortcomings exist for large-scale preparation of transparent wood, such as difficult production, easy warping, and poor cross-grain properties. Moreover, the original three-dimensional structure of transparent wood needs to be retained, and the technological process of delignification needs to be precisely controlled to prevent disintegration of large-scale wood during delignification, which undoubtedly increases cost. Natural fibers have attracted attention as reinforcing polymers with the development of the green economy concept. Compared with synthetic fibers, the mechanical properties of natural fibers are poor, but they have the advantages of low cost and abundance. Among them, jute fiber has attracted attention because of its richness, renewability, low thermal conductivity and high toughness. Jute fibers can be classified into phloem fibers and leaf fibers. Phloem fibers mainly include hemp, jute, flax, ramie, and abutilon, whereas leaf fibers mainly include sisal and banana [15]. In these fibers, the flax cell walls are not lignified, so the length and thickness of the fibers are similar to cotton, which can be used as textile raw materials. Jute, sisal, banana, and other cell walls are lignified, and the fibers are short and hard, which makes them suitable for packaging, sacks, and spinning ropes [16]. Jute fibers are mainly phloem fibers, which is the basic skeleton of plants. Because phloem fibers are highly ordered and crystalline, and the fibers are distributed in a layered structure along the radial direction of the fibers, the mechanical strength of phloem fibers is better. Jute fiber is also widely used in the interior automobile industry as well as the textile industry. The application of composite materials made of jute fibers in automobiles extends from the interior, such as dashboards, to exterior parts, such as the engine hood, body, and structural components [17]. If a single micron diameter jute fiber is used to replace wood by braiding, it can solve the problem of difficult-to-remove lignin and ease of splitting in the transverse direction during preparation of transparent wood.

## 2. Raw Materials and Preparation

### 2.1. Experimental Raw Materials

The main experimental materials are shown in Table 1.

**Table 1.** Main experimental materials.

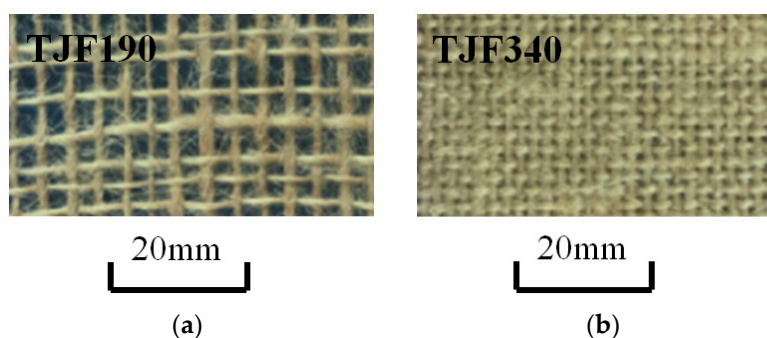
Name	Molecular Formula	Production Company
Jute fiber	–	Zhanjiang Jianqing High-tech Linen Industry Co., Ltd., Zhanjiang, China
Sodium chlorite	NaClO <sub>2</sub>	Aladdin Biochemical Technology Co., Ltd., Shanghai, China
Acetic acid	CH <sub>3</sub> COOH	Aladdin Biochemical Technology Co., Ltd., Shanghai, China
Sodium hydroxide	NaOH	Fuyu Biochemical Technology Co., Ltd., Fuyu, China
Hydrogen peroxide	H <sub>2</sub> O <sub>2</sub>	Harbin Chemical Plant, Harbin, China
Acetone	CH <sub>3</sub> COCH <sub>3</sub>	Fuyu Biochemical Technology Co., Ltd., Fuyu, China
Absolute ethanol	C <sub>2</sub> H <sub>5</sub> OH	Harbin Chemical Plant, Harbin, China
Epoxy resin	–	Wenzhou Tailiqi Company, Wenzhou, China

## 2.2. Preparation of Transparent Jute Fibers

The jute fiber components are shown in Table 2. As shown in Figure 1, sparse and dense jute fibers were selected, and their surface densities are shown in Table 3.

**Table 2.** Jute Fiber components (each component is measured separately) [15].

Components	Jute fiber
Cellulose (wt %)	57–60
Hemicellulose (wt %)	14–17
Lignin (wt %)	18
Pectin (wt %)	14
Waxy (wt %)	–
Ash content (wt %)	5.2
Moisture content (wt %)	9.4

**Figure 1.** Sparse (a) and dense (b) jute fibers.**Table 3.** Surface density of sparse and dense jute fibers.

Jute Fibers	TJF190	TJF340
Surface Density (g/m <sup>2</sup> )	190	340

The two kinds of jute fibers (TJF190 and TJF340) were washed, dried, and placed in a bottle. Sodium chlorite was added to dissolve them (5 wt %, pH 4.6). The reactor was placed in an oil bath to remove the lignin from the jute fibers. The reaction times were 6 and 8 h, and the lignin was heated to 80 °C.

After the reaction, the delignified jute fibers were removed and heated to boiling with 5 mol/L alkaline hydrogen peroxide solution. After 1 h, the solution was cooled to room temperature and freeze-dried. An electronic balance was immersed in anhydrous ethanol solution for 6 h after loading.

Then, epoxy resin and the curing agent were disposed of separately, and the jute fibers were mixed with resin by vacuum impregnation for 2 h. The completely impregnated but not cured jute fibers were sandwiched between two silica gel pads. More than 2 kg of weight was placed over the two silica gel pads to ensure smoothness of the transparent jute fibers. The fibers were dried at room temperature for 24 h.

Figure 2 shows the flow chart of preparing the transparent jute fibers. The jute fibers were cut into squares and washed. The fibers were heated in sodium chlorite solution and boiled in hydrogen peroxide to remove the lignin. After drying, the fibers were impregnated in a mixture of epoxy resin and curing agent. Finally, the fibers were sandwiched between two smooth, flat, dry plates, and the finished transparent jute fibers were cured by air-drying.

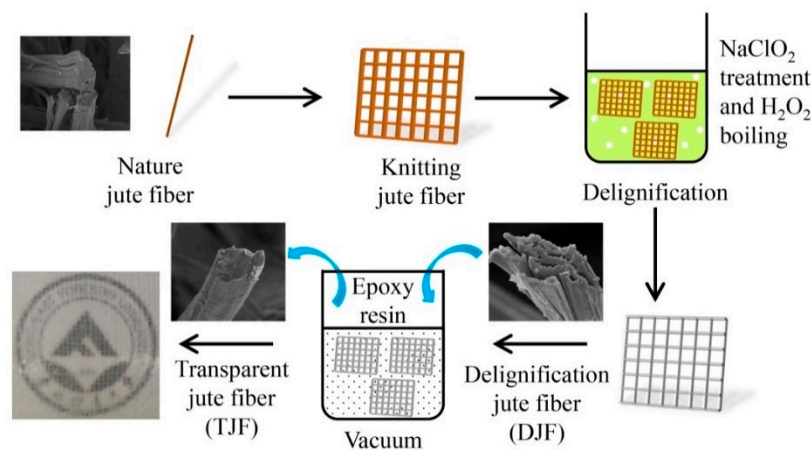


Figure 2. Flow chart to prepare transparent jute fibers.

### 3. Result and Analysis of Transparent Jute Fibers

#### 3.1. Analytical Methods

- A chromatic aberration analysis was performed using an NR110 Handheld Color Aberration Tester (Sanenshi Technology Co., Ltd., Shenzhen, China) to measure the sample. The influence of coconut fiber content on the color of the resin was analyzed using pure epoxy resin as the standard sample.
- The bonding properties of the epoxy resin and jute fibers were analyzed by scanning electron microscopy.
- Transmittance and fog test. According to ASTM D1003: 2007 [18], the edge lengths of the test samples for transmittance and fog were 50 mm. A TU-1901 dual-beam ultraviolet-visible spectrophotometer (Beijing Persee General Instruments Co., Ltd., Beijing, China) was used for the test. The specimens were fixed on the ultraviolet spectrophotometer. Integral spheres were used as accessories and barium sulfate powder was used as the whiteboard.
- Tensile property test. The size of the test spline was 100 mm × 20 mm × 1 mm. A CMT5504 universal testing machine (New Sansi Material Testing Co., Ltd., Shenzhen, China) with a maximum force of 50 kN, was used to determine the temperature and relative humidity of the laboratory at a speed of 5 mm/min. The temperature and relative humidity of the laboratory were 25 °C and 60%, respectively. Five samples of each type were tested.

#### 3.2. Chromatic Aberration Analysis of TJF190 and TJF340

Figure 3 is a comparison of the TJF190 and TJF340 products with pure epoxy resin under an incandescent lamp. Table 4 describes the color difference between the two kinds of jute fibers and the pure epoxy resin in the LAB Uniform Color Space. As a result, the density of the jute fibers increased

and they were brighter, but the overall color was redder and bluer than TJF190. The comprehensive color difference was smaller than TJF190.

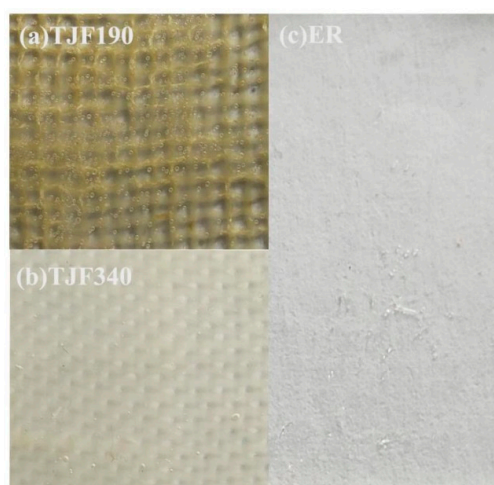


**Figure 3.** Photographs of the TJF190 (a) and TJF340 (b) products and epoxy resin (c) under an incandescent lamp.

**Table 4.** Chromatic aberration of the TJF190/TJF340 products and ER (epoxy resin).

Sample Type	LAB Uniform Color Space			Comprehensive Color Difference $\Delta E$ , $\Delta E = \sqrt{[(\Delta L)^2 + (\Delta a)^2 + (\Delta b)^2]}$
	$\Delta L$ (Light/Shade Difference)	$\Delta a$ (Red/Green Difference)	$\Delta b$ (Yellow/Blue Difference)	
Jute products	-14.62	1.17	4.84	15.44
Ramie products	-16.62	0.71	6.84	17.99

Using pure epoxy resin and curing agent as standard samples,  $L = 76.39$ ,  $a = 0.47$ ,  $b = 1.85$ .

Figure 4 is a comparison of DJF190/DJF340 with the raw materials under an incandescent lamp. Table 5 describes the color difference between the two types of jute fibers and the raw materials in the LAB uniform color space. The brightness difference between DJF340 and the raw materials was greater than that of DJF190. The difference between red and green, the difference between yellow and blue, and the comprehensive color difference was also greater.

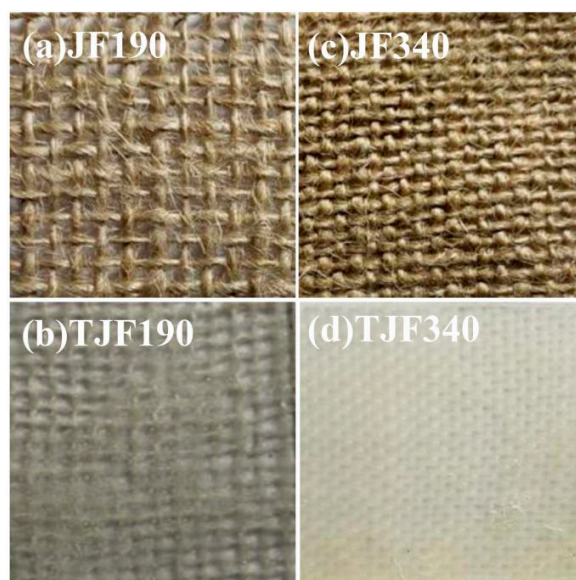


**Figure 4.** Photographs of DJF190 (b) and DJF340 (d) compared with the raw materials JF190 (a) and JF340 (c) under an incandescent lamp.

**Table 5.** Chromatic aberration of DJF190/DJF340 with the raw materials under an incandescent lamp.

Sample Type	LAB Uniform Color Space			Comprehensive Color Difference $\Delta E$ , $\Delta E = \sqrt{[(\Delta L)^2 + (\Delta a)^2 + (\Delta b)^2]}$
	$\Delta L$ (Light/Shade Difference)	$\Delta a$ (Red/Green Difference)	$\Delta b$ (Yellow/Blue Difference)	
Delignification and dense raw material	27.28	−7.85	−8.17	29.54
Contrast raw materials for delignification and jute thinning	17.23	−5.35	−5.03	18.73

Figure 5 is a comparison of the TJF190 and TJF340 products and raw materials under an incandescent lamp. Table 6 describes the color difference between the two jute fibers and the raw material in the LAB uniform color space. As a result, TJF340 was brighter than the raw material, whereas the brightness of TJF190 was lower than that of the raw material. However, the red-green difference, yellow-blue difference, and comprehensive color difference were clearly more obvious in the TJF340.

**Figure 5.** Photographs of TJF190 (b) and TJF340 (d) compared with raw materials JF190 (a) and JF340 (c) under an incandescent lamp.**Table 6.** Chromatic aberration of the TJF190/TJF340 products and raw material.

Sample Type	LAB Uniform Color Space			Comprehensive Color Difference $\Delta E$ , $\Delta E = \sqrt{[(\Delta L)^2 + (\Delta a)^2 + (\Delta b)^2]}$
	$\Delta L$ (Light/Shade Difference)	$\Delta a$ (Red/Green Difference)	$\Delta b$ (Yellow/Blue Difference)	
Comparing raw materials of dense linen products	5.38	−7.59	−15.70	18.25
Raw Material for Ramie Products	−5.72	−5.29	−8.03	11.19

Figure 6 is a comparison of the finished TJF190 and TJF340 products treated with hydrogen peroxide solution (TJF is treated with hydrogen peroxide by default) and treated without hydrogen peroxide solution (UTJF) under an incandescent lamp after removing the lignin. Table 7 describes the color difference between the two types of jute fibers in the LAB uniform color space. As a result,

the brightness difference between the two TJF340 fibers was very significant. The difference between red and green, yellow and blue, and the comprehensive color difference was also quite striking. Use of the hydrogen peroxide solution treatment for TJF190 resulted in no obvious effect on brightness, color, or the other color parameters.

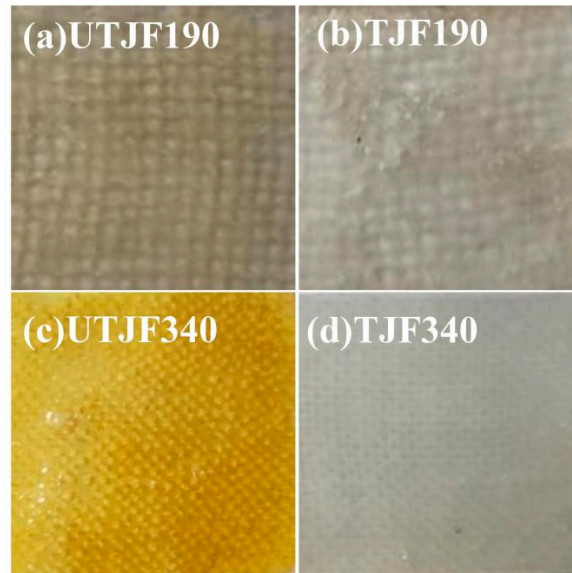


**Figure 6.** Photographs of TJF190 (b)/TJF340 (d) treated with hydrogen peroxide solution and UTJF190 (a)/UTJF340 (c) treated without hydrogen peroxide solution under an incandescent lamp.

**Table 7.** Chromatic aberration of the TJF190/TJF340 products treated with and without hydrogen peroxide solution

Sample Type	LAB Uniform Color Space			Comprehensive Color Difference $\Delta E$ , $\Delta E = \sqrt{[(\Delta L)^2 + (\Delta a)^2 + (\Delta b)^2]}$
	$\Delta L$ (Light/Shade Difference)	$\Delta a$ (Red/Green Difference)	$\Delta b$ (Yellow/Blue Difference)	
Comparisons between dense linen products (without hydrogen peroxide) and hydrogen peroxide solution treatment products	-14.21	2.84	21.97	26.32
Comparing the finished products of sparse jute (without hydrogen peroxide) with the finished products of hydrogen peroxide solution treatment	-0.57	0.11	1.88	1.97

### 3.3. Electron Microscopic Analysis

Before testing, liquid nitrogen was used to wrap the transparent jute fibers and make the transparent jute fibers brittle and fractured to photograph the cross section. A cutting machine was used to cut the transparent jute fibers along the grain to photograph the radial and tangential sections. The specimens were then treated with gold plating by ion sputtering. A JSM-7500F scanning electron microscope (JEOL Ltd., Tokyo, Japan) was used to observe and analyze the cross sections, radial sections, and tangential sections of TJF190 and TJF340. Among them, Figure 7a,b,k,l were magnified 50 times; Figure 7c,d,i,j were magnified 100 times; and Figure 7e,f,g,h were magnified 1000 times.

As shown in Figure 7, the morphologies of the TJF190 and TJF340 jute fibers were quite different at different preparation stages. Figure 7a,b shows the cross-sectional electron microscopic maps of the TJF190 and TJF340 jute fibers, respectively. Figure 7c,d shows the surface electron microscopic maps of the TJF190 and TJF340 jute fibers, respectively. As shown by the figures in the first row, TJF340

was clearly denser than TJF190 at the same magnification, which was consistent with the surface density measurements. Figure 7e is a cross-section of the TJF190 jute fibers after removing the lignin. Many cracks were detected in the TJF190 jute fibers after removing the lignin, which is conducive to resin impregnation. In contrast, the trace amount of lignin removed from the TJF340 jute fibers in Figure 7f was not obvious. Figure 7g,h shows some cracks on the surface of the jute fibers after removing the lignin. Figure 2g also shows some cracks on the surface of the jute fibers, but it is not obvious in Figure 7h. The last row of photographs shows cross sections and the surface of the jute fibers impregnated with epoxy resin. In contrast, the sparse jute fibers in Figure 7i closely combined with epoxy resin. However, the dense jute fibers in Figure 7j were not completely impregnated, due to difficulties removing the lignin and the tight arrangement of the fibers. In summary, the impregnation effect of the epoxy resin was related with the surface density of the jute fibers. Lignin is difficult to remove from jute fibers with a high surface density, and epoxy resin has difficulty entering. However, the tensile strength of dense fibers was still greater than that of sparse fibers, so there is room to improve the dense fibers.

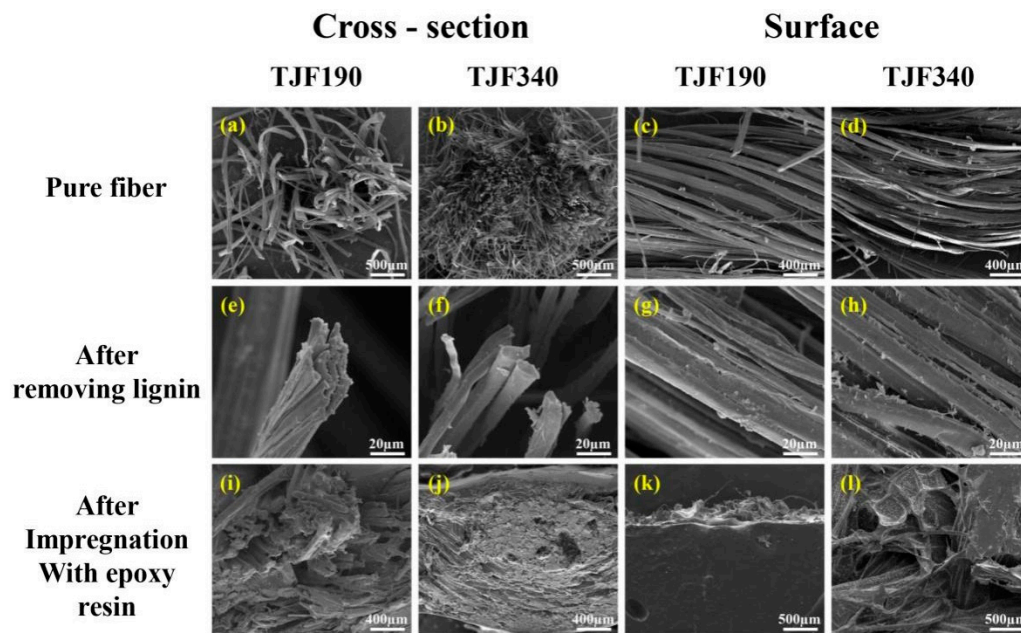


**Figure 7.** Scanning electron micrographs of jute fibers and transparent jute fibers.

### 3.4. Transmittance and Macro-Haze Analysis

Transparent materials become translucent or opaque because they scatter incident light, which is called fog [19]. The prepared transparent jute fibers were photographed at distances of 0, 1, 2, 3, 4, and 5 mm from a school emblem. The haze of the TJF340 was higher than that of TJF190 as shown in the actual photograph of the macro-transparent jute fibers in Figure 8. At a distance of 5 mm from the school emblem, the outline of the school emblem can still be clearly seen through TJF190, while that through TJF340 is relatively blurred. TJF190 and TJF340 were transparent, and the excess rates differed by only 9%. This shows that the density of the transparent jute fibers is proportional to their surface density. The transparent jute fibers with high surface density have a stronger ability to disperse light, so TJF340 has more fog. The school logo blurred gradually from 0 to 5 mm. These photographs show the protection ability of transparent jute fibers for privacy. If it is used as a substitute for glass, it will guarantee personal privacy, while guaranteeing a certain transmittance, which meets the requirement of modern buildings. Moreover, the mist can be changed by adjusting the density of the jute fiber arrangement, which also meets the individualized requirements in the field of interior design.

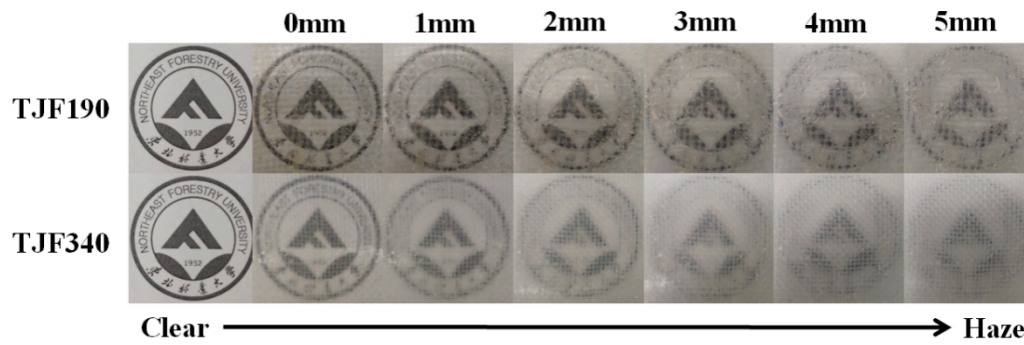


Figure 8. Photographs of TjF190 and TjF340 in the macro-transparent jute fibers.

### 3.5. Tensile Property Analysis

The tensile property analysis is helpful to study the effect of the treatment on biomass-based materials [20,21]. Figure 9 is a comparison of the jute fiber and epoxy resin composites with and without lignin. The epoxy resin–jute fiber (ER–JF) composites were prepared by impregnation with epoxy resin directly without delignification, while Figure 9a,b shows that the tensile strength and modulus of the dense or sparse jute fibers without delignification were slightly higher than the transparent jute fibers. However, Figure 10 shows that the transparent jute fibers had better energy absorption and ultimate elongation after removing the lignin. The dense fibers had higher ultimate tensile strength than the sparse fibers, which is related to the surface density of the jute fibers. The higher the surface density, the higher the tensile strength is. However, sparse fibers have a higher tensile modulus than dense fibers. This may be because the sparse fibers are easier to impregnate with resin, while the dense fibers are more difficult to impregnate, retaining part of the elasticity of the original linen fibers, so strain was greater. Therefore, how to retain strength while providing the optical properties of jute fibers is the focus of future research on transparent jute fibers [22–24].

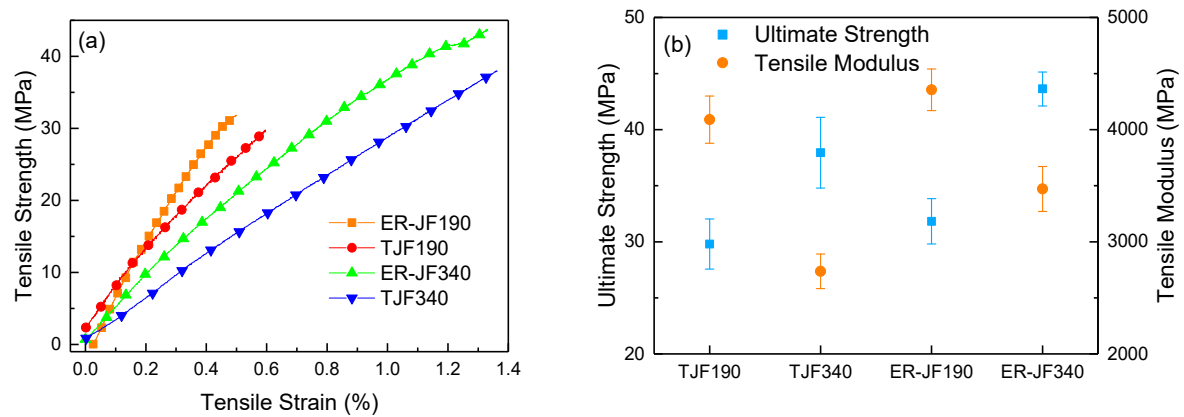


Figure 9. Mechanical properties of epoxy resin–jute fiber (ER–JF) composites: (a) tensile strength–strain curve of four kinds of jute fiber; (b) tensile strength and Young’s modulus of four kinds of jute fiber.

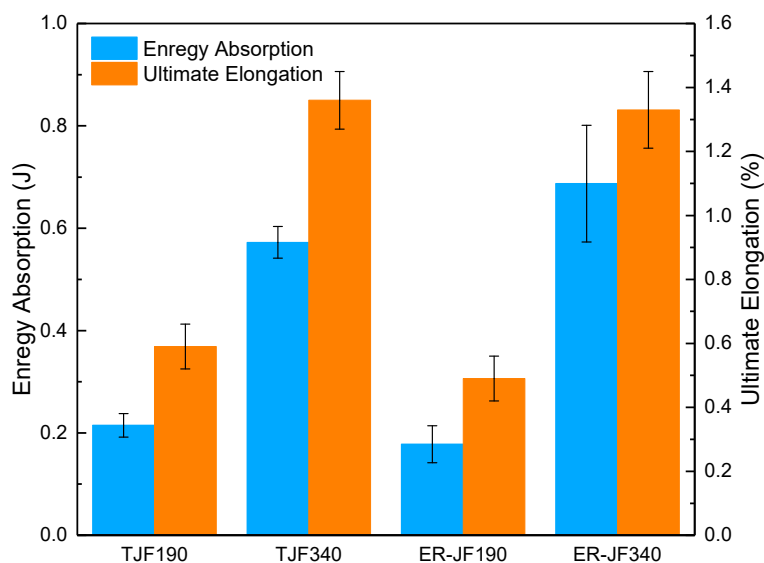


Figure 10. Energy absorption and ultimate elongation of jute fiber composites.

### 3.6. Comprehensive Comparison of Other Transparent Biomass Materials

Tensile strength was compared in transparent coconut fibers (15% TCF), TJF190, and TJF340 with 1 mm transparent balsa wood (TBW) and 15 wt % added (Figure 11). The TBW had the highest transmittance (82%), and its tensile strength was 41.66 MPa. TCF prepared by adding short fibers into the epoxy resin had a transmittance of 60%, but its tensile strength was only 4.55%. The highest transmittance of TJF190 was 60%, while that of TJF 340 was 51%. This result shows that the higher the surface density of the jute fibers, the poorer the transmittance. Transparent jute fibers had lower transmittance compared with transparent wood of the same thickness, but its tensile strength was not inferior. The transmittance of TJF190 was close to that of 15% TCF, but its tensile strength was about seven times that of 15% TCF. Although the transmittance of TJF340 was only 51%, the tensile strength of TJF340 was 43.25 MPa, which exceeded that of TBW. These results show that the mechanical properties of transparent fibers can be effectively improved by knitting the jute fibers.

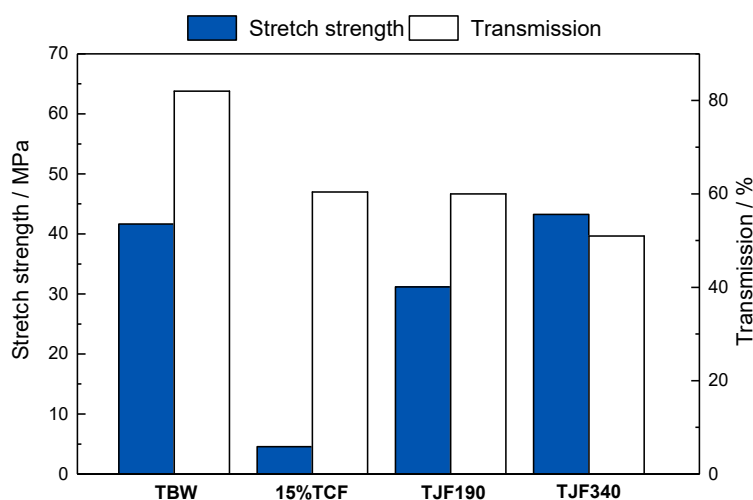


Figure 11. Transparency of transparent biomass materials at 300–800 nm.

## 4. Conclusion

Through a comparative analysis of chromatic aberration, we determined that the brightness difference between the two kinds of TJF340 fibers was very significant (the two are TJF340 products

treated with and without hydrogen peroxide and water after removing the lignin). However, this kind of performance was not prominent in TJF190. Therefore, we conclude that stricter color treatments should be used with denser jute fibers. Otherwise, the finished products will have a great aberration in chroma, which indirectly affects transmittance of the finished products.

In this experiment, we used vacuum impregnation. The gap in the fibers was very large, and the knitting between the fibers exposed many spaces. This phenomenon was more prominent when the lignin was removed. The epoxy resin was used to fill the space occupied by the original lignin, so absolutely no air could enter the gap or space, which required demanding vacuum conditions. Air was continuously pumped out with a vacuum pump in a fully sealed vacuum dryer to create an internal vacuum environment. If a little air is mixed with the jute fibers and epoxy resin, the transmittance and mechanical properties of the whole product are greatly reduced. Therefore, in view of this demanding requirement, we choose the process of impregnating the jute fibers with high pressure vacuum pumping. Only by using this method can transparent jute fibers be produced efficiently in the industry.

The problem of interfacial bonding exists for jute fibers. The highest transmittance of the sparse fibers was 60%, and that of dense fibers was 51%. The maximum tensile strength of the transparent jute fibers was 38.69 MPa, which is much higher than that of TCF with 5% content. These findings show that the tensile strength of jute fibers increased greatly due to the overall braiding of the jute fibers. Delignified biomass fiber materials should be modified in further experiments to enhance their bonding ability with the matrix resin to better conduct stress and improve the mechanical properties of the composites.

The anisotropy of the TCFs and jute fibers was not obvious compared with transparent wood, and the tensile strength of transverse and longitudinal fibers was almost the same, which provides a solution to the problem of transverse splitting of the original transparent wood.

**Author Contributions:** Conceptualization, T.F.; Methodology, T.F.; Software, J.Q.; Validation, T.F. and J.Q.; Formal analysis, Y.S. and L.J.; Investigation, Y.H.; Resources, Y.H.; Data curation, T.F. and J.Q.; Writing—original draft preparation, T.F.; Writing—review and editing, J.Q. and Q.L.; Visualization, Y.H.; Supervision, Y.H.; Project administration, Y.H.; Funding acquisition, Y.H.

**Funding:** This research was funded by Fundamental Research Funds for Central Universities (2572016EBJ1), and the National Natural Science Foundation of China (31470581).

**Conflicts of Interest:** The authors declare no conflict of interest.

## References

1. Qin, J.; Li, X.; Shao, Y.; Shi, K.; Zhao, X.; Feng, T.; Hu, Y. Optimization of delignification process for efficient preparation of transparent wood with high strength and high transmittance. *Vacuum* **2018**, *158*, 158–165. [[CrossRef](#)]
2. Qiu, Z.; Xiao, Z.; Gao, L.; Li, J.; Wang, H.; Wang, Y.; Xie, Y. Transparent wood bearing a shielding effect to infrared heat and ultraviolet via incorporation of modified antimony-doped tin oxide nanoparticles. *Compos. Sci. Technol.* **2019**, *172*, 43–48. [[CrossRef](#)]
3. Fink, S. Transparent wood—A new approach in the functional study of wood structure. *Holzforschung* **1992**, *46*, 403–408. [[CrossRef](#)]
4. Li, T.; Zhu, M.; Yang, Z.; Song, J.; Dai, J.; Yao, Y.; Luo, W.; Pastel, G.; Yang, B.; Hu, L. Wood composite as an energy efficient building material: Guided sunlight transmittance and effective thermal insulation. *Adv. Energy Mater.* **2016**, *6*, 1601122. [[CrossRef](#)]
5. Xu, Y.; Yang, J. Application of light guide lighting technology. *Energy Res. Util.* **2013**, *4*, 45–48. (In Chinese)
6. Li, Y.; Fu, Q.; Yang, X.; Berglund, L. Transparent wood for functional and structural applications. *Philos. Trans. A Math. Phys. Eng. Sci.* **2018**, *2112*, 20170182. [[CrossRef](#)] [[PubMed](#)]
7. Ouyang, J.; Shi, C.; Yuwang, B. Study on “Visual Power” of wood texture. *China Packag.* **2016**, *36*, 31–35. (In Chinese)
8. Yu, Z.; Yao, Y.; Yao, J.; Zhang, L.; Chen, Z.; Gao, Y.; Luo, H. Transparent wood containing Cs<sub>x</sub>WO<sub>3</sub> nanoparticles for heat-shielding window applications. *J. Mater. Chem. A.* **2017**, *5*, 6019–6024. [[CrossRef](#)]

9. Zhu, M.; Li, T.; Davis, C.S.; Yao, Y.; Dai, J.; Wang, Y.; AlQatari, F.; Gilman, J.W.; Hu, L. Transparent wood composites for highly efficient broadband light management in solar cells. *Nano Energy*. **2016**, *26*, 332–339. [[CrossRef](#)]
10. Li, Y.; Yu, S.; Veinot, J.G.; Linnros, J.; Berglund, L.; Sychugov, I. Luminescent transparent wood. *Adv. Opt. Mater.* **2017**, *5*, 1600834. [[CrossRef](#)]
11. Fu, Q.; Yan, M.; Jungstedt, E.; Yang, X.; Li, Y.; Berglund, L.A. Transparent plywood as a load-bearing and luminescent biocomposite. *Compos. Sci. Technol.* **2018**, *164*, 296–303. [[CrossRef](#)]
12. Gan, W.; Xiao, S.; Gao, L.; Gao, R.; Li, J.; Zhan, X. Luminescent and transparent wood composites fabricated by PMMA and  $\gamma\text{-Fe}_2\text{O}_3\text{@YVO}_4\text{:Eu}^{3+}$  nanoparticles impregnation. *ACS Sustain. Chem. Eng.* **2017**, *5*, 3855–3862. [[CrossRef](#)]
13. Wu, J.; Wu, Y.; Yang, F.; Tang, C.; Huang, Q.; Zhang, J. Impact of delignification on morphological, optical and mechanical properties of transparent wood. *Compos. Part A Appl. Sci. Manuf.* **2019**, *117*, 324–331. [[CrossRef](#)]
14. Wang, X.; Zhan, T.; Liu, Y.; Shi, J.; Pan, B.; Zhang, Y.; Cai, L.; Shi, S.Q. Large-size transparent wood for energy-saving building applications. *Chemsuschem* **2018**, *11*, 4086–4093. [[CrossRef](#)] [[PubMed](#)]
15. Jin, J. Research on Jute Fiber Refining Technology. Master's Thesis, Donghua University, Shanghai, China, May 2007.
16. Zhang, R. Study on properties of jute fiber PLA composites. Master's Thesis, Qingdao University, Qingdao, China, May 2011.
17. Jiao, X.; Li, L.; Dong, S.; Wei, C. Mechanical properties of PP/jute fiber composites for automotive interior decoration. *Eng. Plast. Appl.* **2017**, *45*, 13–16. (In Chinese)
18. ASTM D1003-07 Standard Test Method for Haze and Luminous Transmittance of Transparent Plastics; ASTM International: West Conshohocken, PA, USA, 2007.
19. Hsieh, M.C.; Koga, H.; Suganuma, K.; Nogi, M. Transparent cellulose nanopaper. *Sci. Rep.* **2017**, *7*, 41590. [[CrossRef](#)] [[PubMed](#)]
20. Cavallaro, G.; Danilushkina, A.; Evtugyn, V.; Lazzara, G.; Milioto, S.; Parisi, F.; Rozhina, E.; Fakhrullin, R. Halloysite nanotubes: Controlled access and release by smart gates. *Nanomaterials* **2017**, *7*, 199. [[CrossRef](#)] [[PubMed](#)]
21. Cavallaro, G.; Milioto, S.; Parisi, F.; Lazzara, G. Halloysite nanotubes loaded with calcium hydroxyde: alkaline fillers for the deacidification of waterlogged archeological woods. *ACS Appl. Mater. Interfaces* **2018**, *10*, 27355–27364. [[CrossRef](#)] [[PubMed](#)]
22. Yang, W.; Wang, Q.; Li, L.; Hu, G.; Lao, Y.; Ma, H. Surface bacteriostasis of wood-plastic composites modified by ultraviolet grafting. *J. Northeast For. Univ.* **2014**, *10*, 111–114. (In Chinese)
23. Li, X.; Zhou, Z.; Yang, Z. Anti-aging properties of nano-zinc oxide modified wood-plastic composites. *J. Southwest For. Univ.* **2015**, *4*, 81–85. (In Chinese)
24. Wang, Y.; Fu, S. Progress in transparent wood research. *China Pulp & Paper* **2018**, *37*, 68–72. (In Chinese)

